Wastewater matters: Incorporating wastewater treatment and reclamation into a process-based hydrological model (CWatM v1.08)

Journal: Geoscientific Model Development Discussions

Dor Fridman[1], Mikhail Smilovic[1], Peter Burek[1], Sylvia Tramberend[1], Taher Kahil[1]

[1] Water Security Research Group, Biodiversity and Natural Resources Program, International Institute for Applied Systems Analysis (IIASA), Laxenburg, Austria.

Correspondence to: Dor Fridman (fridman@iiasa.ac.at)

Abstract

Wastewater treatment and reuse are increasingly vital for enhancing water use efficiency and ensuring reliable water availability. Wastewater also significantly influences hydrological dynamics within urban watersheds. Although hydrological modeling has advanced to capture human-water interactions, large-scale and multi-resolution models often lack comprehensive integration of wastewater treatment and reclamation processes. This paper presents the new modular wastewater treatment and reclamation module as part of the hydrological Community Water Model (CWatM) and demonstrates its capabilities and advantages in an urban and watershed with intermittent flows. Incorporating wastewater into the model improves model performance by better-representing low- and peak-flows during the dry and wet seasons. It allows for representing wastewater reuse in different sectors and exploring different measures for increasing wastewater reclamation, and its effects on the water stress. Modeling of wastewater treatment and reclamation is relevant for other world regions with similar climates or urbanization patterns, or those promoting wastewater reuse policies. The wastewater treatment and reclamation module is able to scale-up by minimizing the data requirments through a simplified workflows. Combined with the availability of recent datasets of wastewater treatment plants and processes, a global application of the module is feasible. As the current development focuses on water quantity, the water quality dimension of wastewater treatment remains a limitation, which sets the plans of incorporating water quality into the model and developing global input data for wastewater treatment and reclamation.

1. Introduction

Hydrological modeling has developed over the last few decades to account for the human-water interface (Wada et al., 2017). Recent developments in this field focused on developing higher-resolution global hydrological models (GHMs) by increasing models' spatial resolution, adjusting their datasets, and including a variety of water management options (Abeshu et al., 2023; Hoch et al., 2023; Burek et al., 2020; Hanasaki et al., 2022).

Increasing human interventions in the water cycle and higher spatial resolution modeling have emphasized the need to include water management as an integral part of hydrological models (Hanasaki et al., 2022). Some large-scale hydrological models (LHMs) already account for water management aspects, like water withdrawal and consumption, irrigation management, reservoir operations, water transfers, and desalination (Wada et al., 2017). Wastewater treatment and reclamation are other management options that are increasingly important in many regions. Currently, treated wastewater is estimated at 188 km^3 per year globally, which is around 52% of effluents generated. Further, approximately 22% (of treated wastewater) is estimated to be reclaimed (Jones, van Vliet, Qadir, & Bierkens, 2021). Thebo et al. (2017) find that around 35.9 mega hectares of irrigated cropland are supported by rivers dominated by wastewater from upstream urban areas, and Van Vliet et al. (2021) indicate that expansion of treated wastewater uses from 1.6 to 4.0 billion m^3 per month can strongly reduce water scarcity levels worldwide.

Specifically, wastewater reuse is a valuable water source for industrial use and irrigation in water-stressed regions. For example, Israel reclaims around 88% of its treated wastewater, mainly for use in the agricultural sector, where it satisfies about 45% of the agricultural water withdrawals (Fridman, Biran, & Kissinger, 2021). Treated wastewater is also used for irrigation in South European, Mediterranean, and North African countries (Angelakis et al., 1999; Bixio et al., 2006). While accepting exacerbated stress on freshwater resources, the European Parliament is working to improve the quality of wastewater treatment in the EU, aiming to increase wastewater reuse (European Parliament, 2024). It follows that prospects of increased utilization of this resource are plausible. Wastewater collection, treatment, and reclamation are relevant processes for the hydrological modeling of urban catchments and complex water resource systems and are included in different small-scale models (Salvadore, Bronders, & Batelaan, 2015). Large-scale hydrological models often neglect wastewater treatment and reclamation. However, to some extent, few models include wastewater treatment effects on water quality. The Soil & Water Assessment Tool (SWAT) includes septic tanks as an on-site treatment option. It simulates the percolation of wastewater into soils, the interaction between pollutants and the soil media, and bacteria build-up and nutrient uptake (Neitsch, Arnold, Kiniry, & Williams, 2011).

Another example is DynQual, a global water quality model coupled with the PCR-GLOBWB2 hydrological model (Jones et al., 2022). The model includes wastewater treatment processes in water quality simulations while simplifying wastewater treatment and reclamation management. Namely, in DynQual, wastewater is generated, collected, treated, and discharged locally (in a single grid cell).

While these are significant developments, they only partially capture the complex dynamics between human activities and hydrological processes occurring in urbanized catchments or otherwise complex water resource systems.

66 This paper introduces a recently developed, customizable wastewater treatment and reclamation module as part

67 of the Community Water Model (CWatM), allowing various modes of simulating wastewater treatment and

68 reclamation processes.

69 CWatM is a versatile, fully distributed, modular, and open-source hydrological model that simulates natural and

70 human-affected hydrological processes at a daily time step and multiple spatial resolutions ranging from 0.5° to

71 30 arc-seconds (Burek et al., 2020). CWatM has extensive and publicly available documentation of the source

72 code, the model structure, and model training and tutorials (https://cwatm.iiasa.ac.at/, last access: 11 July 2024).

73 The development of the wastewater treatment and reclamation fits with the modularity and flexibility of CWatM

74 by providing various modus-operandi to enable simulation of wastewater treatment and reclamation on global

75 (0.5°), regional (5 arc minutes), and local (up to 30 arc seconds) scales. This paper aims to introduce this module

76 using a high-resolution (around 1 km^2) case study of an urbanized river basin in a relatively dry climate (the

77 Ayalon River basin in Israel).

78 The rest of the paper is organized as follows. Section 2 describes the model development; section 3 covers the

79 case study, input data, and scenarios; and section 4 presents the results, followed by discussion and conclusions

80 in sections 5 and 6, respectively.

81 ## 2. Module development and description

82 ### 2.1. The Community Water Model (CWatM)

83 CWatM is a large-scale distributed hydrological model suitable for implementation at global and regional scales

84 (Burek et al., 2020). It is implemented in the Python programming language and is fully open-source

85 (https://cwatm.iiasa.ac.at). CWatM simulates the main hydrological processes and covers some aspects of the

86 human-water interface. This paper presents the recently developed wastewater treatment module to enhance

87 CWatM's capacities for addressing human water management. The model is applied to the relatively water-scarce

88 Ayalon River basin in Israel. It uses a spatial resolution of 30 arc seconds (~1 km^2 grid) in a geographic coordinate

89 system (WGS84). Groundwater is simulated by the coupled CWatM-MODFLOW6 model (Guillaumot et al.,

90 2022) at a spatial resolution of 500 meters using the UTM36N coordinate system.

91 ### 2.2. Developing the Wastewater Treatment and Reclamation Module (WTRM)

92 The wastewater treatment and reclamation module (WTRM) enhances the capacity of CWatM to simulate the

93 human-water interface at high spatial resolution. It introduces wastewater generation, collection, treatment,

94 discharge, storage, and reclamation to CWatM. Large-scale modeling shall utilize the basic setup of the WTRM

95 for which sufficient data is available globally. Case studies with higher data availability may benefit from optional

96 advanced functions. The following section distinguishes between basic and advanced (optional) functionalities.

97 Figure 1A demonstrates the WTRM workflow, split into three sub-processes: (1) pre-treatment; (2) treatment; (3)
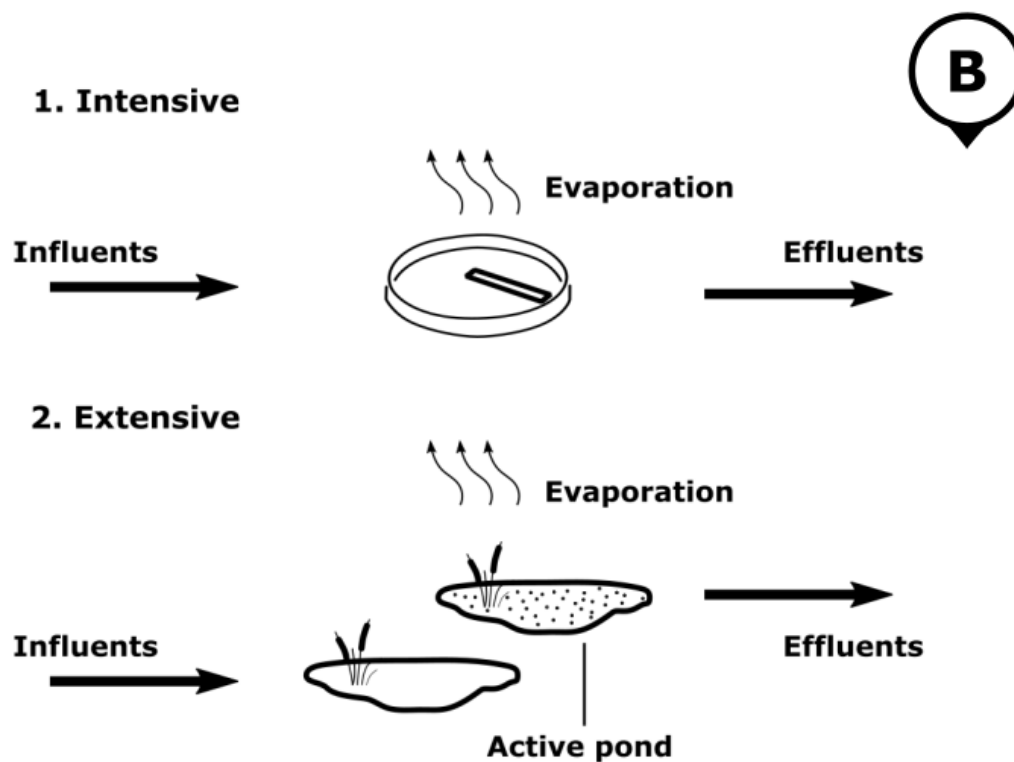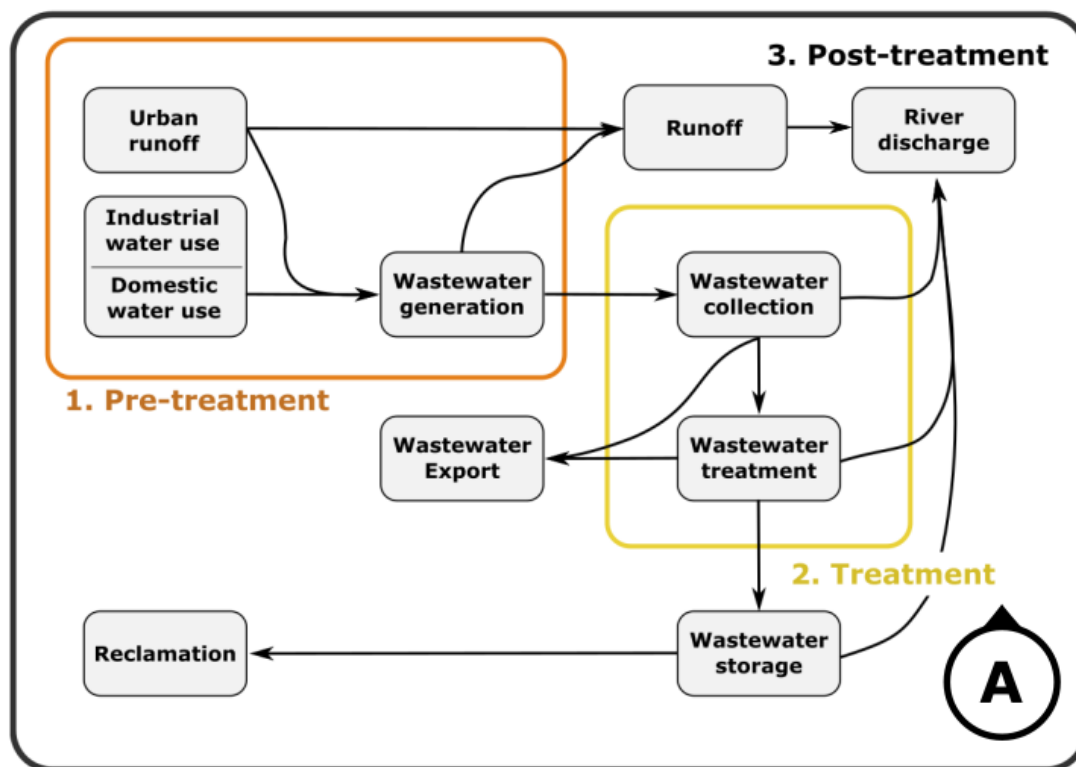
98 post-treatment.

Figure 1: (A) Workflow of the Wastewater Treatment and Reclamation Module, and (B) the main processes and flows in intensive and extensive wastewater treatment systems.

103 **2.2.1. Pre-treatment: wastewater generation and collection**

104 Wastewater generation in CWatM is represented by non-irrigation return flows, which are a function of water

105 availability and sectoral allocation scheme, and the ratio between the consumptive and total water withdrawal.

106 The wastewater module estimates domestic and industrial wastewater generation (Eff^{Dom} and Eff^{Ind}) by multiplying

107 the non-irrigation return flows by the relative sectoral water demand. The next step is to collect and supply

108 wastewater to wastewater treatment plants (WWTP) (see Equation 1).

109

110 **Equation 1: Calculating WWTP influents in WTRM.**

111
$$Inflow_{j,t} = \sum_{l \in j} \left(Eff_{l,t}^{Dom} \times D_j^{Dom} + Eff_{l,t}^{Ind} \times D_j^{Ind} \right) \times Cs_l + Rf_l \times \alpha$$

112 *Note: j* and *t* represent a simulated WWTP and the time step, respectively; *l* indicates a grid cell. Table 4 describes all the WTRM variables,

113 data sources, and default values.

114

115 WWTP service areas (or collection areas) are model input that defines the linkages between the location of

116 wastewater generation (individual grid cells, denoted by *l*) and wastewater treatment plants (denoted by *j*).

117 Wastewater collection is also a function of the sewer connection rate (Cs_l), where a value of one indicates all

118 wastewater is collected and sent to a WWTP. Moreover, it can include urban runoff (Rf_l) due to leakage or

119 integration of the urban stormwater and wastewater systems. The α coefficient defines the system integration level

120 and ranges from zero (no integration) to one (complete systems integration). The total wastewater collected in all

121 grid cells *l* associated with a WWTP *j* is registered as the treatment plant's inflow.

122 Modeling sector-specific WWTP (e.g., treatment of only industrial wastewater) is an advanced model

123 functionality, and to-date does not fit a global application. It uses a boolean variable (e.g., D^{Dom}), which equales

124 one if the treatment plant receives a specific wastewater stream (e.g., domestic). A default value of one for both

125 sectors is set in place in case of missing data.

126 **2.2.2. Treatment: Influent, evaporation, and effluent**

127 Simulated wastewater treatment plants must have the following basic features: location, start year of operation,

128 daily treatment capacity, treatment period (days), and outflow location.

129 Currently, the module supports two optional wastewater treatment technologies that are associated with the

130 treatment period. The two options are intensive and extensive treatment plants, as described in Figure 1b. Intensive

131 treatment refers to the conventional wastewater treatment technology characterized by low residence time and

132 low area requirements. It treats water to secondary or tertiary levels over less than 24 hours (Pescod, 1992).

133 CWatM uses a daily timestep, so the intensive treatment plant's treatment period is set to one day. Any WWTP

134 with a longer treatment period (i.e., >= 2 days) would be classified as extensive. Extensive treatment refers to

135 natural biological systems, consisting of a short primary treatment in a relatively deep anaerobic pond, followed

136 by a longer residence time (20 -40 days) in a shallow facultative pond for secondary treatment (Pescod, 1992).

137 An advanced model feature enables the exceedance of the WWTP daily capacity by temporarily reducing the

138 hydrological retention time (HRT). This feature is enabled by setting a treatment plant-specific minimally allowed

139 HRT, providing WWTP some buffer to handle days with extreme inflows, e.g., due to rain events. Another

140   advanced option is to simulate WWTP closure or upgrades by providing an end-year of operation for a WWTP

141   instance.

142   The main flows within the treatment section are influent, evaporation, and effluent, as described below.

143

144   Influent inflows

145   According to the basic model setup, excess wastewater beyond the plant's daily treatment capacity is discharged

146   to the predefined outflow location (see Table 4). However, the model holds advanced modeling capabilities,

147   enabling WWTP to accept larger inflows to handle temporal fluctuations (e.g., due to significant rain events).

148   Inflows higher than the designed capacity shorten the hydrological retention time (HRT or residence time),

149   resulting in less effective wastewater treatment. The designed retention time is calculated as $HRT_j^{Design} =$

150    $Volume_j/Inflow_j^{Design}$, where $Volume_j$ is the volume of WWTP j, and $Inflow_j^{Design}$ is the daily treatment capacity

151   of WWTP j (Pescod 1992). The daily treatment capacity and time (or designed HRT) are model inputs (see Table

152   4). To allow treatment plants to maintain higher inflows than their designed capacities, the minimally allowed

153   HRT (days) parameter is used. It expresses the lowest operational hydraulic retention time a treatment plant can

154   withstand before it refuses inflows. Following the calculation of the hydraulic retention time, the maximum daily

155   capacity can be calculated as follows $Inflow_{max} = Volume/HRT_{min}$, whereas volume is fixed. For example, a

156   minimally allowed HRT of 0.8 days implies an increase of 25% in the operational daily capacity for a designed

157   treatment time of 1 day.

158

159   Evaporation

160   Water surface evaporation is calculated by multiplying the potential open water evaporation rate with the treatment

161   pools' estimated surface area, and the pool live storage volume limits it. Calculating the surface area of the

162   treatment pools is different for intensive and extensive systems. The surface area of an intensive WWTP is defined

163   as the ratio between the plant volume and the pool depth. For that purpose, a simplified representation of a WWTP

164   treatment pool is adopted based on a clarifier design (used during both primary and secondary treatment; Pescod,

165   1992), and the pool depth is estimated at 6 meters (WEF, 2005; see Figure B1).

166   Extensive systems are modeled as natural biological treatment ponds, alternately filling up and treating water.

167   These processes consist of a relatively short anaerobic treatment in deeper ponds followed by a long-term (20-40

168   days) residence in facultative shallow ponds (see Figure 1B; also refer to Pescod, 1992). Unlike intensive systems,

169   treatment ponds in extensive systems may remain empty for long periods. Since evaporation is simulated at the

170   pond level, it considers only ponds with positive water storage.

171

172   **Equation 2: calculation of the surface area of extensive treatment systems.**

173
$$As_j = \frac{1}{Depth_j} \times \left(VolCap_j \times \frac{TreatTime_j}{TreatPool_j - 1} \right)$$

174

175   The surface area of each treatment pool is calculated by dividing the pool's volume by its depth (see Equation 2;

176   *Depth*, currently set to 1.5 meters, as the depth of a facultative pond; Pescod, 1992). Each pool volume is derived

6

177 by multiplying the daily capacity (*VolCap*) with the pool filling time. The latter is a function of the designed

178 treatment time (*TreatTime*) and a predefined number of treatment pools (*TreatPool*; currently set to two; Pescod,

179 1992). Although evaporation losses are overall small (see Figure 4), we allow modelers to change these default

180 technical values with their estimates (see Appendix B).

181

182 Effluents

183 Treated wastewater (effluents) are discharged into a natural water body or sent to reservoirs for reclamation. The

184 timing of effluent release differs between intensive and extensive systems. Figure 1B shows the main differences

185 between these two types of systems. In intensive systems, influents remain in the treatment plant throughout the

186 predefined treatment time. For example, for a treatment time of one timestep, the effluent volume at time *t* equals

187 the influent volume minus evaporation of time *t – 1*.

188 Extensive systems differentiate between two types of treatment ponds. At each time, one treatment pond receives

189 all inflows, and the other pond is either full or empty. Ponds that do not receive inflows and are not empty are

190 considered 'active', i.e., in which wastewater treatment occurs. Effluents are released from 'active' ponds under

191 any of the following conditions: (a) the predefined treatment time has passed since the 'active' pond stopped

192 receiving inflows; (b) all pools are at full capacity, and more influents should be added into the system. In the

193 latter case, the effluents always originated from the 'active' pond that had gone through the longest treatment time,

194 though they may not be fully treated.

195 ### 2.2.3. Post-treatment

196 The basic module has two post-treatment options: river discharge and reclamation. Direct reclamation (e.g., for

197 irrigation purposes) is possible using the CWatM reservoirs and water demand routines. This option requires data

198 on the linkages between WWTP and reservoirs, representing existing or planned water conveyance systems. The

199 routine iterates over the list of WWTP-Reservoir links and attempts to send treated wastewater to associated

200 reservoirs. In the case of multiple receiving reservoirs, the water is split in proportion to the reservoirs' remaining

201 storage (calculated as $remainingStorage_{i,t} = totalVolume_i - liveStorage_{i,t}$). Access water is discharged on

202 predefined overflow locations if all related reservoirs are full. Discharge into streams/rivers is the default behavior

203 if no reservoir is associated with a treatment plant. Finally, untreated wastewater is discharged if a plant's inflows

204 exceed the plant's peak capacity (see minimally allowed HRT in section 2.2.2).

205 Treated wastewater can be managed in a separate reclamation system by establishing a set of artificial, off-stream

206 (type-4) storage reservoirs. A type-4 reservoir is not connected to the river network, thus having no channel-

207 related inflows or outflows. Instead, water inputs include water/wastewater pumping, and water outputs are

208 evaporation and pumping. The model combines the two approaches mentioned above, as each WWTP can be

209 linked to one or more reservoirs or discharge its water directly into a river channel. Indirect reclamation can be

210 simulated by releasing the water into a channel, upstream to a lift area where river water is abstracted and used,

211 or into a reservoir linked to the river network, where effluents are mixed with fresh water.

212 The module is designed to allow inter-basin transfers of wastewater or treated wastewater, yet this advanced

213 option is not required in the case of a global model. Interbasin transfer of treated wastewater aims to account for

214 cases in which the reclamation areas extend beyond the borders of the simulated river basin. In that case, WWTP-

215 specific export-share parameters indicate the daily fixed percent of treated wastewater transferred for reclamation

7

216 in other basins. Similarly, the interbasin transfer of un-treated wastewater represents cases in which treated
217 wastewater collected in one basin is treated in another. It occurs automatically if a defined service area is not
218 associated with any WWTP within the simulated basin.

219 ## 3. Case study application

220 Israel is located on the Eastern Coast of the Mediterranean between the latitudes 29°N –34°N and along the 35°E
221 longitude. Its Central coastal and Northern parts are governed by a Mediterranean climate (hot and dry summer),
222 its Eastern parts are arid due to rain shadow from its Central Mountain range, and the Southern parts experience
223 a semi- to hyper-arid climate due to their vicinity to the world's desert belt.

224 During the 1960s, Israel initiated a country-wide water conveyance system (the 'National Water Carrier') to
225 transfer water southwards from the northern Sea of Galilee, allowing rural development and large-scale irrigation
226 in the semi-arid Negev region (Tal, 2006). Israel's water system is intensively managed today and relies primarily
227 on seawater desalination, treated wastewater reclamation, and groundwater abstraction. Although it is a nationally
228 managed system, significant regional differences exist in sectoral water provision (Fridman et al., 2021).

229 The Ayalon basin is in central Israel and the West Bank and stretches 815 km^2 between the western slopes of the
230 Judea Mountains and the Mediterranean Coastal zone. A few kilometers inland, the Ayalon spills into the Yarkon
231 stream (see Figure 2). Ayalon is an urbanized river basin partially overlaying the Tel Aviv-Yaffo metropolitan
232 area downstream and the city of Modi'in in its middle segment. Downstream urban areas result in considerable
233 water demand, vast runoff from sealed areas, and a high rate of wastewater generation. Upstream, the landscape
234 of the Ayalon basin is predominantly a rural mosaic of open areas and small settlements. Patches of irrigated
235 agriculture and forests are primarily found in the South-Eastern parts of the basin.

236 Ayalon is a seasonal river originating in the South-Eastern part of the basin. An artificial 'horseshoe' shaped
237 reservoir ('Mishmar Ayalon') regulates its flows and maintains relatively fast groundwater recharge. Five main
238 tributaries drain the remaining basin and feed the Ayalon River downstream. An artificial cemented canal collects
239 the river water before crossing densely populated urban areas downstream.

240 ### 3.1. Data sources

241 The CWatM provides global datasets at 0.5 degrees and 5 arc-minutes, as Burek et al. (2020) described. This high-
242 resolution analysis better combines global and local data sources to represent the case-study hydrologic processes
243 and human-hydrologic interactions (Hanasaki et al., 2022). Table 1 provides an overview of both the global (e.g.,
244 meteorological forcings, soil characteristics, topography, and the river network) and the local datasets (e.g.,
245 wastewater treatment and reclamation, reservoir networks, aquifer properties, landcover maps, seawater
246 desalination, and water demand). A complete documentation of the dataset associated with this publication is
247 available at https://doi.org/10.5281/zenodo.12752967.

248

249 **Table 1: Model inputs from global and local datasets. Unless explicitly indicated, all datasets were resampled to 30 arc-**
250 **seconds or converted to a raster format.**

Input data	Spatial (temporal) resolution	Data sources and comments on data processing

8

Global datasets		
Meteorological forcings	0.5° grid (daily) Downscaling to 30 arc-seconds (multi-annual monthly average)	ISIMIP 3a, GSWP3-W5E5 (Lange, Mengel, Treu, & Büchner, 2022) WorldClim (Fick & Hijmans, 2017)
Soil	30 arc-seconds grid (fixed value)	Dai et al. (2019) Shangguan, Hengl, Jesus, Yuan, & Dai (2017)
Topography	3 arc-seconds grid (fixed value)	MERIT Digital Elevation Model (Yamazaki et al., 2017)
River network properties flow direction map	30 arc-seconds grid (fixed value)	MERIT Hydro IHU (Eilander et al., 2020)
Local/modified datasets		
Landcover maps	500 meters grid (annual)	MODIS Global landcover between 2001 -2019 (Friedl & Sulla-Menashe, 2019), OpenStreetMap (Urba areas, water, and green spaces; available at https://www.openstreetmap.org), Ministry of Agriculture and Rural Development (MOAG, 2022; cultivated land), and Hamaarag (2017; forests' map)
Municipal and industrial water demand	Local government borders, polygons (annual)	Israel Central Bureau of Statistics (ICBS, 2022). A Random Forest regression imputed missing data for different localities and specific years. Palestinian Central Bureau of Statistics (PCBS, 2022).
Wastewater treatment plants' data base: WWTP location, outflow location treatment levels, years of operation service areas, connection rate, and wastewater generation coefficients	Point data (fixed value) Tabular format (by year) Local government borders, polygons (fixed value)	A national dataset was compiled mainly relying on a report by the Israel National Reserve Authority (INRA, 2016) and data from PCBS (2022a).
Desalination	National value (annual)	Annual desalination capacity between 2005 - 2019 (Gov.il, N.D.). A basin-scale desalination is allocated proportionally to the relative domestic water demand. For example, the national supply of desalinated seawater in 2005 and 2015 was 20

		and 503.4 MCM, respectively. In the same years, the Ayalon desalinated seawater supply is estimated at 3.4 and 88 MCM.
Reservoirs	Digitized polygons and attributes (fixed value)	Manually identify and digitize reservoirs based on aerial photography and satellite imagery. Depth and volume were assumed based on fieldwork and engagement with water managers. The link between WWTP to reservoirs is based on INRA, (2016).
Groundwater basin and aquifers Aquifer borders Aquifer properties – coastal/mountain	Digitized polygons (fixed value) Digitized polygons (fixed value)	Aquifer maps were taken from Israel Hydrological Services (2014), and porosity and permeability were taken from Melloul et al. (2006) for the coastal basin and from Wollmann, Calvo, & Burg (2009) for the mountain basin.

251

Groundwater basins and aquifers

253 This case study uses the coupled CWatM-MODFLOW6 model to account for the interface between surface and
254 groundwater hydrology and groundwater dynamics (Guillaumot et al., 2022). The Ayalon River basin lies above
255 two principal groundwater aquifers. The west mountain aquifer is part of the larger Yarkon-Taninim aquifer
256 system and has two partially separated sub-aquifers reaching a thickness of 600 meters. It comprises carbonate
257 sedimentary rocks and has a relatively high but non-homogenous hydraulic conductivity (Wollmann, Calvo, &
258 Burg, 2009). The slopes of the West Judea mountains function as recharge zones, and the top layers in the Western
259 foothills are made of chalk and marl and act as an aquitard, confining the Western Mountain aquifer (see Figure
260 A1). To the west, the relatively shallow Coastal aquifer (thickness up to 200 meters) mixes a sandstone aquifer
261 with a clay lens, resulting in varying hydraulic conductivity (Melloul, Albert, & Collin, 2006). Data on
262 groundwater abstraction volumes, locations, and the water table changes was unavailable.

263

Reservoirs

265 We have manually identified and digitized reservoirs in the Ayalon basin using multiple data sources, including
266 georeferenced aerial photography, visual inspection of satellite imagery, fieldwork, and interviews with local
267 water management experts. The biggest reservoir in the Ayalon basin is Mishmar Ayalon (7.5 MCM; Figure 2),
268 a seasonal water storage fed by the upstream section of the Ayalon River and regulates downstream flows. The
269 Natuf reservoir is located on a prior quarry site northeast of the basin (4.3 MCM) and contributes to groundwater
270 recharge. Four smaller reservoirs constitute the wastewater irrigation infrastructure and have a total designed
271 storage of 634,200 m^3. This reclamation system extends beyond the basin's borders, for which we account by
272 exporting a fraction of the treated wastewater.

273

Wastewater in the Ayalon basin

Two primary wastewater treatment plants collect wastewater generated in the main cities, and small-scale treatment plants collect those generated in the rural sector. The *Shafdan* WWTP treats all wastewater generated in the Tel Aviv-Jaffa metropolitan area in the adjacent Sorek basin, which is out of the scope of this analysis. Later, they were exported to the North-Western Negev for irrigation purposes (Fridman et al., 2021). The Ayalon WWTP is the most significant facility in the basin, with a daily capacity of 81,000 m^3. It collects treated wastewater from the cities of Lod and Modi'in (see Figure 2) and their surroundings. An extensive treatment plant has existed since 1995, but development and population growth have exceeded its capacity, increasing sewer discharge frequency into the stream. An intensive activated sludge treatment plant with a daily capacity of 54,000 m^3 started operating in 2003. However, on some occasions, the daily inflow exceeded the daily capacity by over 1.5 times (see Table S4). Almost ten small-scale wastewater treatment plants in the Ayalon basin are treating sewers at a settlement scale with a total daily capacity of 12,298 m^3.
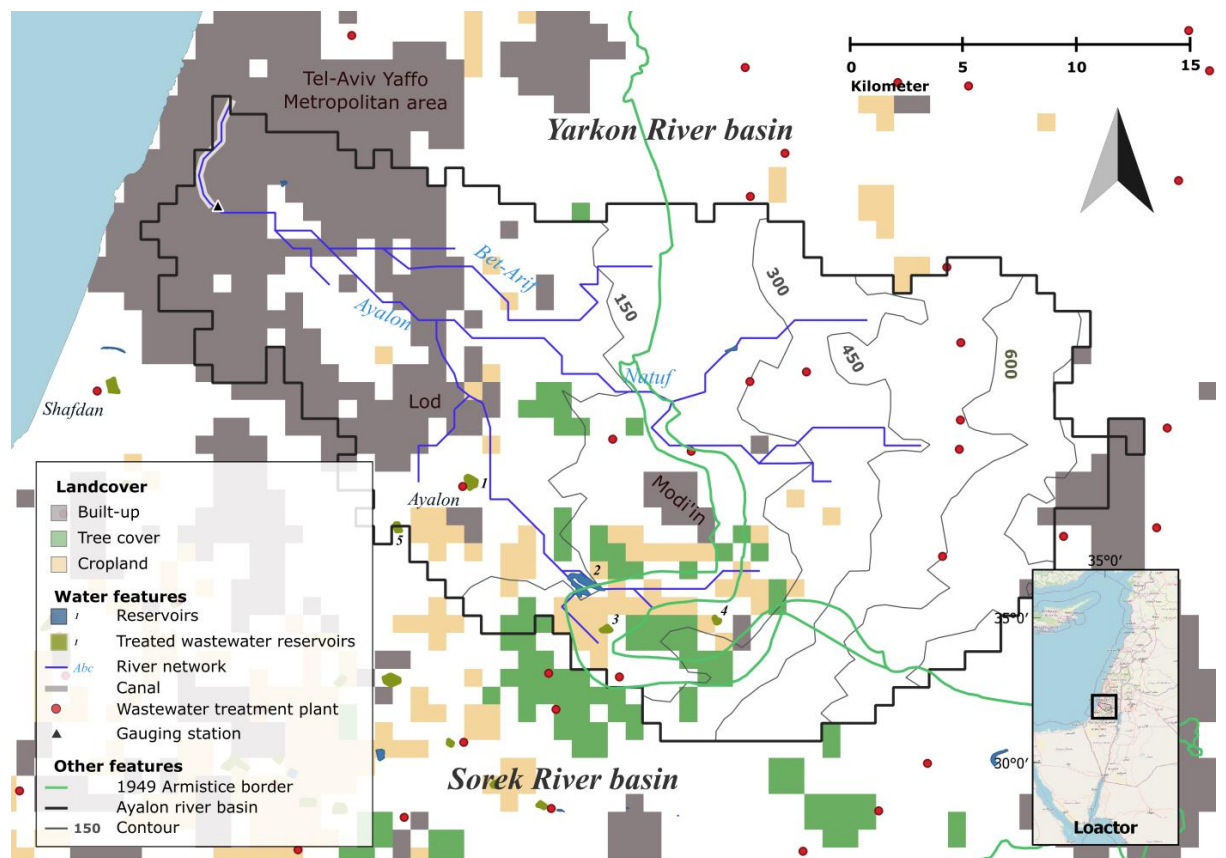

Figure 2: the Ayalon River basin case study: land cover and significant water features. Partially uses data from © OpenStreetMap contributors 2022. Distributed under the Open Data Commons Open Database License (ODbL) v1.0. Marked reservoirs: (1) Ayalon; (2) Mishmar Ayalon; (3) Ta'oz; (4) Mesilat Zion; (5) Mazli'akh.

3.2. Setting calibration scenarios and model parameters

In this analysis, we simulate the Ayalon basin hydrology and wastewater treatment and reclamation under three different scenarios, aiming to explore the effects of the wastewater treatment module's different modes of operation on model calibration and basin-scale water resource management. In the first scenario (S0), we disable the wastewater treatment and reclamation module. The second (S1) and third (S2) include wastewater treatment

11

297 and reclamation without and with urban runoff collection, respectively. The share of urban runoff flowing into

298 the sewers is set as a calibration parameter in S2. Additional calibration parameters are associated with

299 evapotranspiration rates of irrigated croplands and grassland, soil depth adjustment, within grid-cell soil moisture

300 spatial distribution, soil hydraulic conductivity and water content at saturation, Manning's roughness coefficient,

301 riverbed exchange rate, urban evaporation coefficient, and urban infiltration coefficient. The emphasis on the

302 urban landscape is due to the relatively high share of built-up areas in the Ayalon basin (see Figure 2).

303 We set three more wastewater reclamation scenarios apart from calibration scenarios by expanding the irrigated

304 agriculture area (by 2.5%) and increasing storage volume (by 5%) for two reservoirs for which command areas

305 are defined: Ayalon and Mazlikh. One scenario includes expansion and increased storage, and each of the two

306 scenarios includes expansion or increased storage.

307   **4. Results**

308   **4.1. Model validation**

309 We have calibrated the Ayalon case study against the daily average discharge at the Ayalon-Ezra gauging station

310 (34.794° E, 32.04° N; Figure 2) over the period August 1st, 2001, to July 30th, 2006, and validated over the period

311 August 1st, 2007 to December 31st, 2019. We further compared the simulated evapotranspiration with multiple

312 satellite-derived products (Figure S6; Mu et al., 2014; Reichle et al., 2022; Rodell et al., 2004) and the simulated

313 monthly influent flows into the Ayalon WWTP with observed data between 2016 -2019 (Figure 5; Ayalon Cities

314 Association, 2021). We measure model performance using the Kling-Guphta Efficiency (KGE) and Nush-

315 Sutcliffe equilibria (NSE) coefficients (Moriasi et al., 2015).

316 The S2 (wastewater and urban runoff collection) scenario generated the best-performing model (KGE = 0.76;

317 NSE = 0.72 during training), followed by S1 (wastewater without urban runoff collection; KGE = 0.27; NSE =

318 0.61), and S0 (KGE = -0.4; NSE = 0.57). Model performance is lower during the validation periods across all

319 scenarios. During the validation periods, the complete implementation in scenario S2 also resulted in the best-

320 performing model ($KGE_{2006-2013} = 0.69$, $KGE_{2014-2019} = 0.55$). Over the complete simulation period (1995 -2019),

321 the mean observed discharge at the outlet is 0.81 m^3 s^{-1}, and it was best matched by the simulated discharge in

322 scenario S2 (0.87 m^3 s^{-1}; see Table 3). The full implementation scenario (S2) best matches the observed discharge

323 also during most of the days in the dry (April-September) and the wet season (Figure 3). Sometimes, the model

324 overestimates discharge or simulates flow events during the dry period (e.g., late April 2003, see Figure 3). This

325 is often associated with a mismatch between forcing data (e.g., precipitation) and actual precipitation (see Figure

326 S5 and Table S1).

327 The simulations were compared with different remote-sensing derived evapotranspiration (RS-ET) time-series.

328 All scenarios can capture seasonal dynamics quite well but overestimate ET during early spring (around March-

329 April, except SMAP; see Figure S6). The 'No wastewater' (S0) scenario highly overestimates the ET, whereas the

330 other two (S1, S2) scenarios better align with the RS-ET data, particularly after 2015. There are differences

331 between RS-ET datasets associated with process, forcings, and parameterization errors (Zhang et al., 2016); some

332 are shown in Table S2. GLDAS v2.1 shows the lowest KGE across scenarios, and SMAP indicates the highest

333 (see Table S3). These findings are consistent with an intercomparison of RS-ET datasets (Kim et al., 2023).

334   Furthermore, the fitness to RS-ET time-series improves when additional features of the wastewater module are

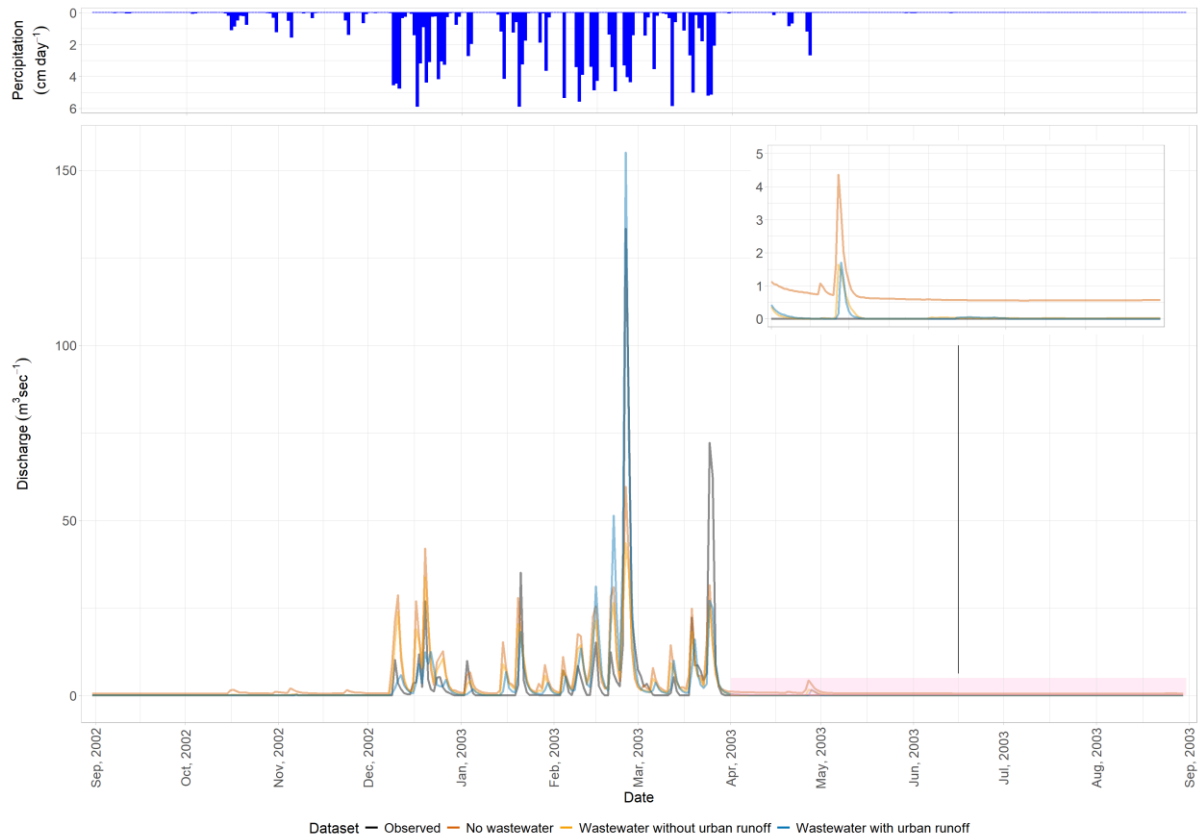335   incorporated across all datasets. The average KGE is -0.68 (S0), -0.27 (S1), and -0.17 (S2).

336

337   **Figure 3: comparison of the observed and simulated discharge at the outlet across scenarios during a selected year**
338   **(September 2002 -September 2003).**

339   Modeling the intermittent Ayalon River case study is challenging, mainly due to its arid climate and small basin

340   area. Under these conditions, even a small deviation in the absolute simulated discharge results in a high relative

341   error. It follows that diverting return flows (i.e., sewage) away from the river was a crucial step in the Ayalon

342   model calibration. Introducing wastewater treatment and reclamation into CWatM enables simulating actual water

343   dynamics in the Ayalon basin, resulting in a better-performing model. The KGE values of scenarios S0-S2

344   between 1995 and 2019 are -0.75, 0.17, and 0.66, and the percentage differences between the simulated and

345   observed average discharge are 162%, 62%, and 4.1%, respectively (see Table 3). Similar improvement is also

346   shown when comparing simulated and observed discharge between 1995 and 2019 (see Figures S1, S2, and S3).

347   The improvement from including the wastewater treatment and reclamation module (scenario S1) is associated

348   with reducing the dry season's baseflow from an average of 0.07 m^3 s^{-1} to 0.06 m^3 s^{-1}. The effects of urban runoff

349   collection were mainly evident in the wet season's discharge, which was reduced from an average of 2.53 m^3 s^{-1}

350   (scenario S1) to 1.68 m^3 s^{-1} (scenario S2). The collection of urban runoff into the sewers reduces flows downstream

351   to urban areas and fits, to some extent, the inflow dynamics into the Ayalon wastewater treatment plant (see Figure

352   5).

353   **Table 3: Model performance under different scenarios over the complete simulation (1995 -2019). The dry season**
354   **occurs from April to September.**

13

Scenario	KGE (during calibration)	NSE (during calibration)	Annual mean discharge (% relative to observed)	Dry season's mean discharge (% relative to observed)	Wet season's mean discharge (% relative to observed)
Observed	-	-	0.81 ± 4.9 (-)	0.04 ± 0.38 (-)	1.59 ± 6.9 (-)
S0: No wastewater	-0.75 (-0.4)	0.55 (0.55)	2.12 ± 5.1 (162%)	0.7 ± 0.85 (1650%)	3.54 ± 6.92 (123%)
S1: Wastewater without urban runoff collection	0.17 (0.27)	0.62 (0.61)	1.3 ± 4.36 (62%)	0.09 ± 0.65 (125%)	2.53 ± 5.9 (59%)
S2: Wastewater with urban runoff collection	0.66 (0.76)	0.7 (0.72)	0.87 ± 4.1 (7%)	0.06 ± 0.42 (50%)	1.68 ± 5.67 (6%)

355

356   **4.2. Component and flows of the wastewater module**

357 The wastewater flows between different model components are illustrated in Figure 4 using the water circle

358 concept, a simplified representation of the water cycle (Smilovic et al., 2024). Wastewater treatment plants'

359 inflows mainly consist of domestic sewage mixed with urban runoff (e.g., in dual-purpose urban drainage

360 systems). In the Ayalon basin case study, the largest share (68%; circle A) of the influents is being treated in the

361 *Shafdan* WWTP outside of the basin of interest (i.e., sewage exported; also see Figure 2), and approximately 14%

362 are sent to reservoirs for reclamation. The remaining share includes the discharge of treated wastewater (4%) and

363 raw sewage (8%). Evaporation loss from WWTP is marginal (<4%) and is represented by one of the unlabeled

364 wedges on the wastewater circle.

365 In Israel, treated wastewater is operated separately from potable water, and reclamation reservoirs do not receive

366 stream inflows; instead, they only store treated wastewater. About 46% of the reservoirs' inflows in the Ayalon

367 basin are of treated wastewater (circle B). A large share of the total inflows is lost to evaporation (16%), and

368 approximately 8% is reclaimed for irrigation.

369 Figure 4 (circle C) shows that the Ayalon basin water supply heavily relied on groundwater abstraction (96%).

370 However, it has been slowly replaced by desalinated seawater, reaching an average share of 60% annually between

371 2015 and 2019. In comparison, wastewater reclamation only plays a minor role (approximately 2% of the water

372 use). Nevertheless, treated wastewater satisfies about 10% of the basin's effective irrigation. Wastewater

373 reclamation in other basins also relies on sewage generated in the Ayalon basin, as all the wastewater from the

374 Tel-Aviv metropolitan area is treated in the *Shafdan* WWTP and used for irrigation in the South of Israel (Fridman
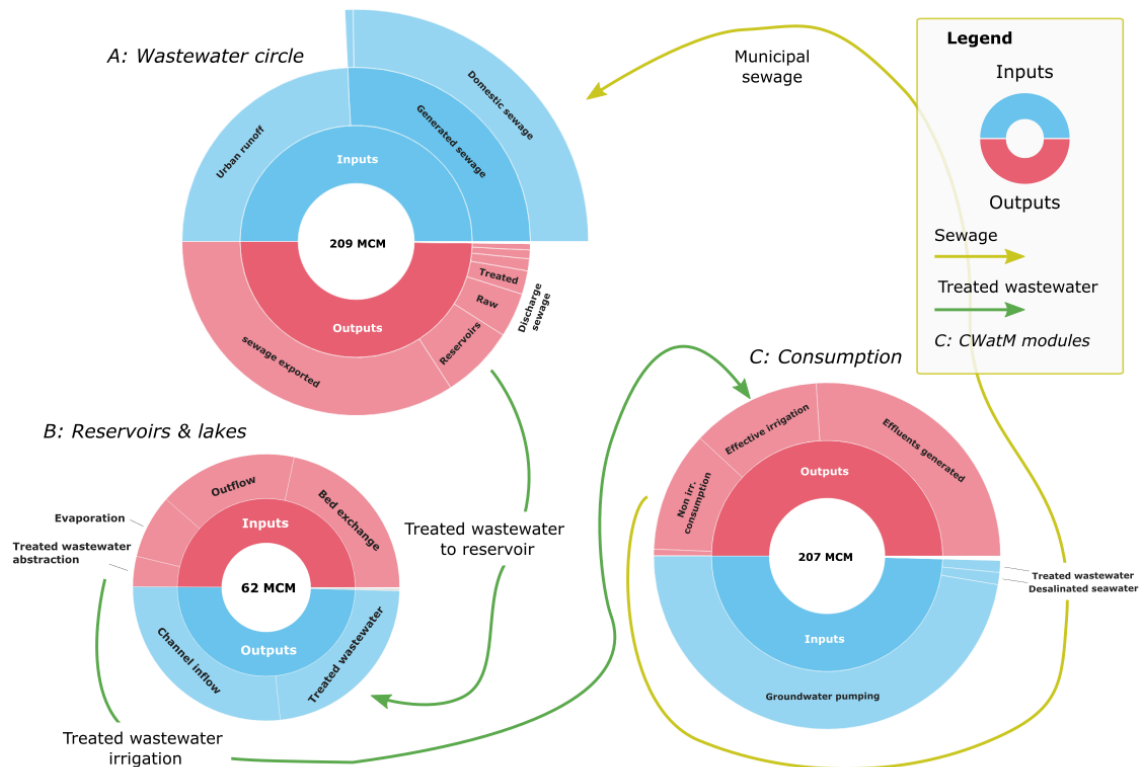
375 et al., 2021).

376

14

Figure 4: Average annual sewage and treated wastewater flows within and between CWatM modules, based on a simulation for the Ayalon River Basin, Israel, from 1/1/2001 -30/07/2006.

4.3. Modeling wastewater and urban stormwater collection systems

CWatM includes two main hydrological processes for urban areas: return flows (e.g., sewage generation) and urban runoff. These flows are managed by either separated or combined collection and drainage systems. In Israel, two systems are operated separately to collect urban wastewater and stormwater. However, stormwater frequently leaks into the sewers due to illegal connections of urban drainage.

The runoff collection coefficient allows the user to control the magnitude of systems integration. One combined system would have a coefficient of one, implying all urban runoff flows into the sewers collection system, and a coefficient of zero suggests two completely separated systems. The calibrated model ended up with a coefficient of 0.78, implying that 78% of urban runoff flows into the sewers.

The advantages of the runoff collection coefficient are shown in Figure 5, comparing the monthly inflows to the Ayalon WWTP against the simulated inflows with (S2) and without (S1) urban runoff collection. On average, between 2016 and 2019, the Ayalon WWTP accepted 1,780 +/- 86 thousand m^3 sewers every month. The average inflows in the scenarios without and with urban runoff collection are 1,562 +/- 119 and 1,699 +/- 203 thousand m^3 per month, respectively. Overall, the model underestimates the inflow to the Ayalon WWTP, as shown in the top panel of Figure 5, during the dry months (e.g., April to June), which is probably due to the use of annual model inputs for water withdrawal, that do not capture seasonality. Seasonality is only captured by the 'Wastewater with urban runoff' (S2) scenario as a direct result of urban runoff collection. Another factor limiting WWTP inflows is the minimally allowed HRT presented in section 2.2.2. Sensitivity analysis implies that a one percent change in the parameter value results in an average 0.23% change in the WWTP inflows (see Supplementary Information and Figure S8).

15

Rain events during the wet season often result in increased inflows into the wastewater treatment plants (e.g., during December 2016 or January 2018). The scenario that includes urban runoff collection (S2) can simulate these peaks, though it slightly overestimates them, whereas no peaks are simulated for scenario S1, where no urban runoff is collected (see Figure 5 bottom panel). While it may be that the runoff collection parameter was set at a value that is too high, overestimating the peak flows can also result from errors in precipitation data (see Figure S5). The wastewater with urban runoff collection (S2) scenario performs the scenario without wastewater collection based on multiple parameters (showing lower bias and higher NSE and correlation; see Table S5).
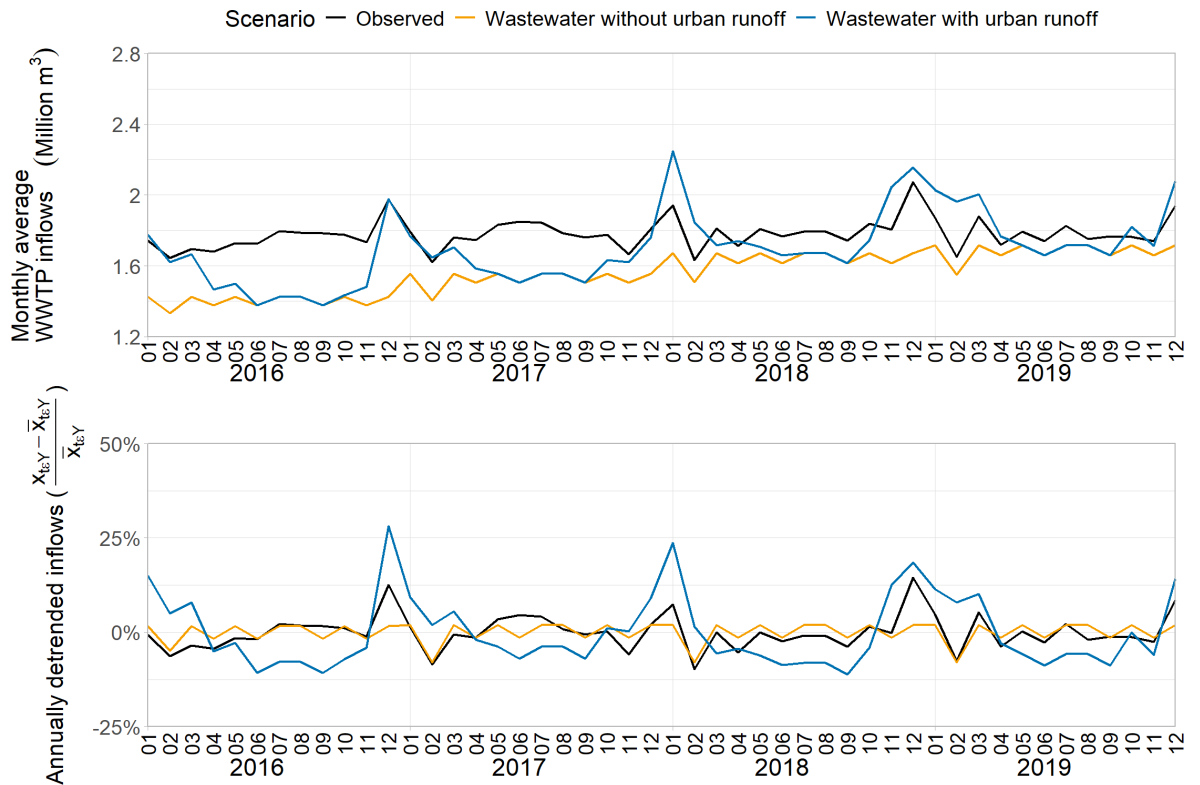

Figure 5: Observed VS. simulated monthly wastewater inflows into the Ayalon WWTP with and without urban runoff collection using absolute values (top chart) and annually detrended values (bottom chart).

4.4. Modeling of wastewater reclamation potential and impacts

Wastewater treatment and reclamation may significantly affect water management, particularly for complex water resource systems in water-scarce countries. Israel is a water-scarce country that reclaims wastewater, utilizes desalination water, and transfers water between river basins to mitigate water stress. As Israel manages water nationally, analyzing water resources on a basin scale aligns differently from Israel's actual state of water resources. Instead, the following scenarios aim to illustrate the relevance of the WTRM module to water resource management.

Until the early 2000s, the Ayalon River basin's water supply relied primarily on groundwater abstraction. As a result of population growth and the expansion of the Ayalon WWTP's daily treatment capacity in 2003 (from 22,000 to 54,000 m3/day), the simulated wastewater reclamation has nearly doubled, increasing from 1.5 million m^3 in the year 2000 to 2.7 million m^3 in 2005. In the same year, desalinated seawater was first supplied, satisfying approximately 3% of the total water demand in the basin. Over the years, the role of desalination increased,

16

accounting for around 47% of the water supply. The share of treated wastewater slightly increased, reaching 2.7% (approximately 3 million m^3), compared with 1.5% in 2000. Most importantly, avoided groundwater pumping in 2010 enhanced Israel's water security by reducing the pressures on aquifers, and the avoided seawater desalination reduced energy-for-water use and water production costs (Fridman et al., 2021).

Focusing on the Ayalon WWTP's reclamation projects (see Figure S9), Table 3 presents the multiannual average absolute and relative wastewater reclamation (for irrigation) between 2000-2010. Overall, there is little difference between the baseline and agricultural expansion scenarios, showing a slight increase in the reclamation volume but a slight decrease in the relative wastewater irrigation (relative to irrigation demand). These findings point out a balanced proportion between storage and water demand. Small access storage is kept, allowing additional irrigation to respond to increased water requirements. The two scenarios, which include increasing storage, demonstrate higher wastewater reclamation volume (4.7%-4.9%) and relative irrigation increasing from 17.3% to 17.8-18.1%. The share of wastewater reclamation out of the total irrigation demand increases from around 13% to 18% in 2000 and 2003, respectively, and reached almost 25% in 2006 (see Figure S10). These changes were associated with an increased capacity of the Ayalon WWTP in 2003 and precipitation variability, e.g., lower irrigation requirements during wet years compared with a relatively constant supply of treated wastewater. As this reclamation project extends southwards, outside the Ayalon River basin, the model also estimates further reclamation of almost 2 million m^3 (i.e., treated wastewater sent for reclamation outside the basin). In addition, more than 50 million m^3 are collected and treated in the *Shafdan* WWTP southwest of the Ayalon river basin (see Figure 2) and are almost entirely reclaimed.

Table 3: Average and standard deviation of the absolute and relative wastewater reclamation in the reclamation project of the Ayalon WWTP between 2000-2010.

Scenario	Wastewater reclamation, thousands m³ (share increase relative to baseline)	Wastewater irrigation (% of total irrigation)
Wastewater and urban runoff collection (Baseline)	2,423.4±536.8 (-)	17.3±4.1%
Agricultural expansion and increased reservoir capacity	2,543.1±514.4 (4.9%)	17.7±4%
Increased reservoir capacity	2,536.7±515.3 (4.7%)	18.1±3.9%
Agricultural expansion	2,447.2±507.4 (1%)	17±4%

5. Discussion

Wastewater treatment and reclamation play a crucial role in the hydrological modeling of urban watersheds, especially in low-discharge/intermittent rivers.

447 Discharges from wastewater treatment plants often dominate urban watersheds' hydrological signals, increasing
448 low-flows, flashiness, and the frequency of medium and high-flow events (Coxon et al., 2024). The effect of
449 wastewater on stream hydrological signals would become more pronounced in intermittent streams, challenging
450 model calibration. Acknowledging this fact, one may compromise on model performance in urban watersheds,
451 yet including wastewater treatment and reclamation in the modeling allows for increased model performance as
452 it better represents local water management processes. The example provided in this paper demonstrates this point
453 by showing a significant increase in model performance due to including wastewater treatment and reclamation
454 in the modeling.

455 To our knowledge, only a few existing hydrological models account for wastewater treatment and reclamation.
456 Dyn-Qual, for example, simplifies the treatment process and only allows for indirect reclamation, i.e., treated
457 water is discharged into rivers and can be abstracted downstream. SWAT model represents wastewater treatment
458 by including pit latrines, yet both models focus on the water quality and missing critical operations associated
459 with water quantity (e.g., reclamation through reservoirs or directly to fields). Although addressing the highly
460 relevant topic of water quality, the representation of wastewater processes in these two models would not
461 contribute to model calibration in urban or intermittent watersheds.

462 The importance of including wastewater treatment and reclamation in high resolution (i.e., ~1km) hydrological
463 modeling is also aligned with recent findings, as these models are susceptible to the effects of human activity on
464 the water cycle and often require better representation of these processes and more precise data (Hanasaki et al.,
465 2022). It follows that the WTRM complements the recent shift towards high-resolution modeling at global (van
466 Jaarsveld et al., 2024) and more local scales (e.g., CWatM implementation in Bureganland Austria; Bhima River
467 Basin, India; North China; Guillaumot et al., 2022; Yang et al., 2022).

468

469 **The wastewater treatment module utilizes multiple features of CWatM, providing tools to conduct policy-**
470 **relevant analysis on water resources management and wastewater treatment and reclamation.**
471 Wastewater is increasingly perceived as an untapped resource and is marked as a potential water source to reduce
472 water stress or drought risk. Hydrological models, such as CWatM, are often used to inform decision-making and
473 policies for enhancing water resource management and can benefit from WTRM capabilities.

474 The WTRM interacts with different existing modules and routines in CWatM. The analysis described in this
475 manuscript demonstrates such interactions with three additional processes. The source-sector abstraction fraction
476 and reservoir operation options are pivotal in modeling the treated wastewater reclamation. The former can define
477 the desired water mix, restricting wastewater reclamation by some sectors (e.g., forbidding households from using
478 treated wastewater). The reservoir operations options are used during the direct reclamation.

479 Indirect reclamation is enabled when treated wastewater is released into a river channel or a reservoir, diluted,
480 and is later abstracted downstream, and direct reclamation is mediated through a designated reservoir,
481 disconnected from the river network (type-4 reservoirs). The inflows into this reservoir consist only of water
482 transfers, and the outflows are limited to abstraction and evaporation losses. The water levels in these reservoirs
483 are not affected directly by river flows and runoff, and they can maintain a traceable stock of treated wastewater
484 over the long run. Abstraction from reservoirs occurs either within a certain buffer (i.e., defined by the number of
485 grid cells) from the reservoir or within the area of an associated command area (area served by the reservoir
486 regarding water supply). Combined with the source-sector abstraction fraction, the modeling of the Ayalon basin

487   has limited the use of treated wastewater for irrigation and livestock to a smaller extent. Other existing uses, like

488   urban landscaping or cooling of thermal powerplants, were ignored, as data was unavailable.

489   Utilizing these modules and processes, the manuscript explores the potential effects of increased storage of

490   wastewater reclamation reservoirs and expanding irrigated agriculture areas. It focuses on the command areas

491   associated with two reclamation reservoirs (as indicated in Figure S9), indicating a high share of irrigation with

492   treated wastewater (~17%). The module variables could be utilized for exploring a wide variety of water

493   management instruments, including using treated wastewater to mitigate drought risk (conveying and storing

494   treated wastewater in high drought risk areas), to recharge the aquifer (controlling reservoir infiltration rate), or

495   explore pathways for agricultural expansion/intensification. Wastewater reclamation can also have economic or

496   environmental benefits. The Ayalon case study is relevant for both due to potentially avoided seawater

497   desalination, which is more expensive and requires more energy. Economic, resource intensity, and emission data

498   from different sources (e.g., life cycle assessments; see Liao et al., 2020; Meron et al., 2020) could complement

499   such analysis, applying a Nexus perspective.

500

501   **Flexible model design and available global datasets provide a robust starting point for simulating**

502   **wastewater treatment and reclamation scenarios at a global scale and coarser resolutions. Some data gaps**

503   **remain and provide opportunities for scientific engagement.**

504   The Community Water Model, as well as other large-scale hydrological models (Hanasaki et al., 2022; Hoch et

505   al., 2023), is shifting towards a multi-resolution modeling framework, allowing users to work on a global scale

506   with coarser resolutions and on a local scale with higher resolutions. The need to better represent wastewater

507   treatment and reclamation in global, regional, and local hydrological modeling is linked to its increasing potential

508   as a water resource. The WTRM provides diverse tools for including wastewater treatment and reclamation into

509   hydrological modeling. So far, the manuscript has focused on the module's advanced mode of operation, which is

510   suitable for data-abundant regions or local case studies where data collection efforts are feasible. Nevertheless,

511   applying the WTRM at coarser (e.g., 5 arc-minutes) spatial resolution globally or in data-scarce regions requires

512   a simplified workflow and a global data inventory.

513   Following the CWatM modular and flexible structure, the WTRM was developed with that notion in mind,

514   facilitating a simple mode of operation with minimal data requirements but including advanced processes when

515   data is available. The results presented and discussed show a significant increase in model performance as a result

516   of a more straightforward implementation of the module (i.e., without urban runoff collection), which, together

517   with the reclamation scenarios, point to the potential impact of upscaling the analysis to cover other urbanized

518   watersheds and water-stressed regions. The recent development of different global datasets provides an

519   opportunity for upscaling this analysis, though these data would have to undergo some processing to fit the

520   CWatM data structure. Hydrowaste (Ehalt Macedo et al., 2022) is a global WWTP dataset describing plants'

521   location, treatment level, operational status, population served, overflow discharge point, and daily capacity. It

522   was recently used to determine the impact of droughts on water quality (Graham et al., 2024) and to account for

523   the global microplastic fiber pollution from laundry (Wang et al., 2024). Second, Jones et al. (2021) compiled a

524   global gridded dataset (at a 5 arc minutes resolution) describing wastewater generation volumes and collection,

525   treatment, and reclamation rates. The data has already been used to force global studies on water quality (van

526   Vliet et al., 2021).

19

These two datasets provide sufficient global data at a spatial resolution of 5 arc minutes to accommodate six of the seven mandatory variables required to setup a simple simulation (see Table 4). However, data is lacking for the year of establishment (or the start of operation) of a WWTP, which could be assumed by utilizing auxiliary time-series data, like drinking water sanitation and hygiene (WASH) available from the joint monitor program (JMP, at https://washdata.org), or sectoral outputs from monetary input-output tables (e.g., https://worldmrio.com). These data could cast temporal trends of increased sanitation coverage or sectoral economic activity. Two additional challenges are indicated in Table 4, associated with the treatment days and service (wastewater collection) area. Following Ehalt Macedo et al. (2022), the latter can be traced back from the WWTP to serve the nearest, most likely upstream, population centers. Treatment days are associated with the WWTP classification into intensive and extensive, which can be associated with location and economic factors (like GDP per capita or electrification status). The availability of such data at national, sub-national, and grid scales deems the classification of WWTP as intensive or extensive and feasible.

Advanced simulations are not pursued globally, so data sources for their required variables are not sought, except for reclamation and reservoir connections, as reclamation significantly impacts model performance and water resource management analysis. The reclamation rates estimated by Jones et al., (2022) can be used for that purpose. However, as it is not linked to any specific WWTP or reservoir, as required by the WTRM, it would require some pre-processing and simplifying assumptions. Some ongoing efforts to identify potential wastewater reclamation for specific WWTP can support this processing (Fridman et al., 2023), yet both data sources would involve high uncertainties at the grid scale. Two other approaches could be taken to assess different reclamation scenarios, including indirect reclamation from waterbodies (e.g., rivers and lakes) or simulating on-site type-4 reservoirs with command areas set as fixed buffers. Such reclamation scenarios could be used to explore reclamation by other non-agricultural sectors.

Table 4: Model variables for simple and advanced simulations and potential data sources. Note: * indicates the variable is unavailable but could be concluded by utilizing auxiliary data; ** indicates the variable is unavailable but could be estimated based on published methods; * indicates available data is highly uncertain at grid scale and can be used to inform scenarios.**

Model variable	Simulation mode	Description [Default value]	Potential Data source
Location	Simple	Geographic location (longitude, latitude) of WWTP [-]	Ehalt Macedo et al., 2022
From year	Simple	The first year of a WWTP operation; as an advanced option, one may include the last year of operation (i.e., the closing of a treatment plant) or trigger several instances of a treatment plant (i.e., upgrade) [-]	Not available*
Volume	Simple	Daily capacity of the WWTP in cubic meters [-]	Ehalt Macedo et al., 2022
Treatment days	Simple	Duration of treatment in days (retention time by design) is associated with treatment technology: intensive treatment (1 day) or extensive	Ehalt Macedo et al., 2022*

		(approximately 30 days), as described in the manuscript [Intensive: 1 day; extensive > 1 day]	
Collection (service) area	Simple	Service area of different WWTPs, e.g., grid cells with water consumption which are connected to a given WWTP, indicated as WWTP ID [-]	Ehalt Macedo et al., 2022**
Collection share	Simple	Share of sewage generated, collected, and sent to WWTP, i.e., rate of connection (0 -1) to WWTP [-]	Jones et al., 2021
Overflow	Simple	Geographic location (longitude, latitude) of the discharge point from WWTP into waterbodies (rivers, lakes, ocean) [-]	Ehalt Macedo et al., 2022
Export share	Advanced	Share of treated wastewater used outside of the basin (0 -1; do not apply to global simulations) [0]	-
Contributing sectors	Advanced	Sectors from which wastewater is treated in a given WWTP (boolean 0/1) [1 for all sectors]	-
Min_HRT	Advanced	The minimally allowed hydrological retention time ranges between 0.001 -number of treatment days. This indicates how much additional water can be accepted daily over the daily capacity, e.g., in case of rain events or high water consumption. A value of 0.001 results in a potential inflow multiplier of 1,000, and a value equal to the treatment days results in no access inflows [treatment days]	-
Reclamation and WWTP connection to reservoirs	Advanced	Links between WWTP and reservoirs and the rules for reuse of wastewater by different sectors [-]	Jones et al., 2021***

553

6. Conclusions

555   Wastewater primarily affects the hydrology in urbanized watersheds, particularly in water-stressed regions.
556   Wastewater reuse can ease the pressure on natural water sources and reduce drought risk. However, large-scale
557   hydrological models do not account for wastewater treatment and reclamation. The recent trend towards higher
558   spatial resolutions further emphasizes the need to include local data and processes in hydrological modeling.
559   This paper introduces a novel wastewater treatment and reclamation module integrated into the large-scale multi-
560   resolution Community Water Model. It provides a range of operational modes to balance modeling needs and data
561   availability worldwide. A high-resolution case study of an urbanized and water-stressed watershed illustrated the

562 WTRM's added value in terms of enhanced model performance and the inclusion of additional water sources,
563 such as reclaimed wastewater. The role of wastewater in water resource management planning can now be
564 included in hydrological simulations, often used to inform such policies. Recently published global datasets were
565 mapped to model variables, indicating that global modeling at coarser spatial resolution (e.g., 5 arc minutes) is
566 also feasible. Some remaining data gaps, including the lack of time-series or missing information on reclamation
567 projects, would require some assumptions and additional processing of input data. The compilation of a global
568 input dataset is one desired future development. As wastewater is naturally associated with water quality, this
569 aspect remains a limitation within the scope of the current development and would also be addressed in future
570 developments.
571
572

7. Appendices

Appendix A

Figure A1 describes the vertical and lateral permeability of the YARTAN and coastal aquifers in Israel. The

coastal aquifer forms a relatively narrow stripe stretching North to the South. Next, the western mountain aquifer

is located towards the east, showing a relatively diverse permeability. The YARTAN groundwater basin includes

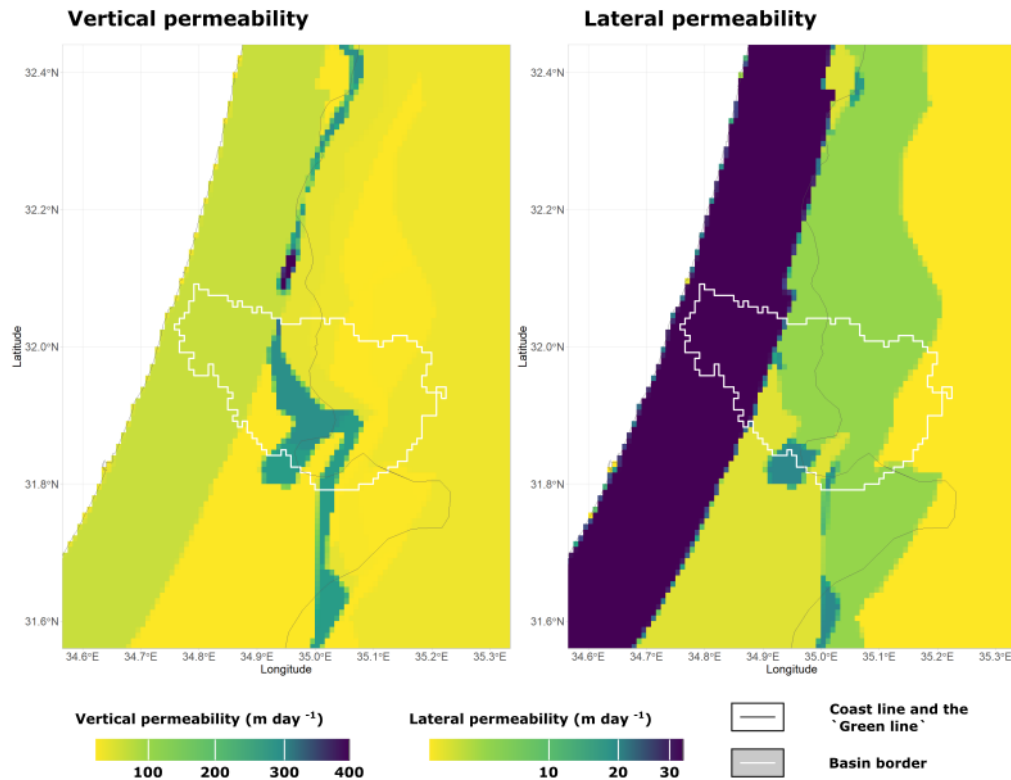the western mountain aquifer but extends far beyond the borders of the Ayalon River basin.

Figure A1: Vertical and lateral permeability in the YARTAN and Coastal aquifers in the Ayalon basin and its
surroundings.

Appendix B

The treatment pool depth in an intensive WWTP represents the depth of a clarifier through which sewage flows

at different treatment stages. The ratios between the clarifier's depth and diameter are relatively fixed, with the

aim of optimizing sewers' biological treatment (e.g., bio-film development). A standard design for a clarifier is a

relatively deep pool with a sloped bottom, as demonstrated in Figure B1. In the WTRM, the pool depth is only

used to calculate the water surface area and simulate evaporation losses, and therefore, we find a simplified

representation of the treatment pool with a flat bottom sufficient. In Figure B1, we convert the sloped bottom

clarifier dimensions (WEF, 2005) to the equivalent pool depth in a flat clarifier, maintaining the pool's volume.

This results in an approximate depth of 6.6 meters, which, based on data collected for the Ayalon case study, was

rounded to 6 meters. We allow modelers to change the pool depth of either intensive, extensive, or both treatment

systems by using the following settings in the settings file: 'pooldepth_intensive', 'pooldepth_extensive'. The

default settings are hard coded as 6 and 1.5 meters, as described in this manuscript. In addition, to calculate the

596　evaporation from extensive WWTP, we allow users to change the default value of two treatment pools by adding

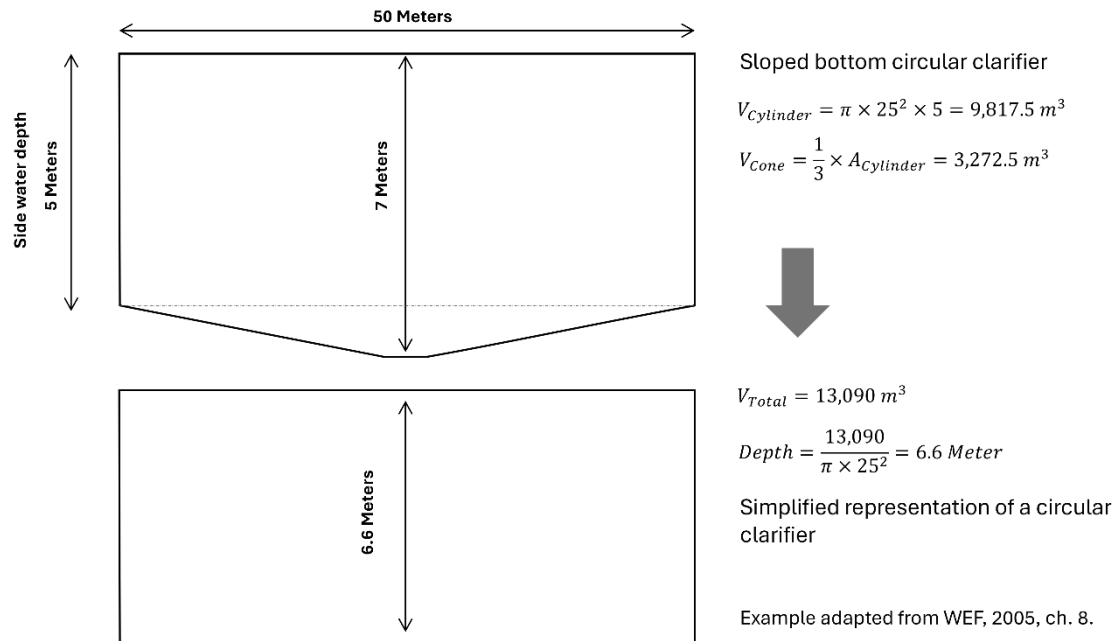597　the 'poolsExtensive' to the settings file.

598

Sloped bottom circular clarifier

$$V_{Cylinder} = \pi \times 25^2 \times 5 = 9{,}817.5 \ m^3$$

$$V_{Cone} = \frac{1}{3} \times A_{Cylinder} = 3{,}272.5 \ m^3$$

$$V_{Total} = 13{,}090 \ m^3$$

$$Depth = \frac{13{,}090}{\pi \times 25^2} = 6.6 \ Meter$$

Simplified representation of a circular clarifier

Example adapted from WEF, 2005, ch. 8.

599　**Figure B1: A simplified approach to estimate wastewater treatment pools depth in an intensive WWTP.**

8. Code and Data Availability

601　The complete model (CWatM-Israel v1.06.1) used to conduct the simulations presented in this manuscript is

602　available from https://doi.org/10.5281/zenodo.13990296 (last accessed: 25/10/2024). The input data used for this

603　publication, including model settings and initial conditions files, can be downloaded from

604　https://zenodo.org/doi/10.5281/zenodo.13990451 (last accessed: 25/10/2024). The Community Water Model

605　(CWatM) manual can be accessed via https://github.com/iiasa/CWatM.

9. Author contributions

607

608　DF, MS, and PB developed the module code (Wastewater treatment and reclamation), and prepared model input

609　and observation datasets. DF, MS, and PB have prepared model inputs. DF performed the simulations and

610　associated post-processing, and prepared the paper with contributions from MS, PB, ST, and TK. MS, ST, and

611　TK acquired the funding and were in charge of project administration and supervision.

10. Competing interests

613　The contact author has declared that none of the authors has any competing interests.

24

11. Disclaimer

Any opinions, findings, and conclusions or recommendations expressed in this material do not necessarily reflect the views of the funding organizations..

12. Financial support

13. References

Abeshu, G. W., Tian, F., Wild, T., Zhao, M., Turner, S., Chowdhury, A. F. M. K., Vernon, C. R., Hu, H., Zhuang, Y., Hejazi, M., and Li H.: Enhancing the representation of water management in global hydrological models. *Geoscientific Model Development*, *16*(18), 5449–5472. https://doi.org/10.5194/gmd-16-5449-2023, 2023.

Angelakis, A., Marecos Do Monter, M. H. F., Bontoux, L., and Asano, T.: The status of wastewater reuse practice in the Mediterranean basin: need for guidelines. *Water Res.*, 33(10): 2201-2217. https://doi.org/10.1016/S0043-1354(98)00465-5, 1999.

Ayalon Cities Association.: Wastewater treatment plant Ayalon-Nesher - Annual report for 2019. https://ayalonb.co.il, last access: 3/10/2024, 2020

Ayalon Cities Association.: Wastewater treatment plant Ayalon-Nesher - Annual report for 2020. https://ayalonb.co.il, last access: 3/10/2024, 2021

Ayalon Cities Association.: Wastewater treatment plant Ayalon-Nesher - Annual report for 2021. https://ayalonb.co.il, last access: 3/10/2024, 2022

Ayalon Cities Association.: Wastewater treatment plant Ayalon-Nesher - Annual report for 2022. https://ayalonb.co.il, last access: 3/10/2024, 2023

Bixio, D., Thoeye, C., de Koning, J., Joksimovic, D., Savic, D.,Wintgens, T., and Melin, T.: Wastewater reuse in Europe. *Desalination*, 187(1): 89-101. https://doi.org/10.1016/j.desal.2005.04.070, 2006.

Burek, P., Satoh, Y., Kahil, T., Tang, T., Greve, P., Smilovic, M., Guillaumot, L., Zhao, F., and Wada, Y..: Development of the Community Water Model (CWatM v1.04) – a high-resolution hydrological model for global and regional assessment of integrated water resources management. *Geoscientific Model Development*, *13*(7), 3267–3298. https://doi.org/10.5194/gmd-13-3267-2020, 2020.

Coxon, G., McMillan, H., Bloomfield, J. P., Bolotin, L., Dean, J. F., Kelleher, C., Slater, L., and Zheng, Y.: Wastewater discharges and urban land cover dominate urban hydrology across England and Wales, EGU General Assembly 2024, 14-19 Apr 2024, EGU24-5850, https://doi.org/10.5194/egusphere-egu24-5850, 2024.

Dai, Y., Xin, Q., Wei, N., Zhang, Y., Shangguan, W., Yuan, H., Zhang, S., Liu, S., and Lu. X.: A Global High-Resolution Data Set of Soil Hydraulic and Thermal Properties for Land Surface Modeling. *Journal of Advances in Modeling Earth Systems*, *11*(9), 2996–3023. https://doi.org/10.1029/2019MS001784, 2019.

European Parliament.: New EU rules to improve urban wastewater treatment and reuse (News: press releases, published 10-04-2024). https://www.europarl.europa.eu/news/en/press-room/20240408IPR20307/new-eu-rules-to-improve-urban-wastewater-treatment-and-reuse#:~:text=EU%20countries%20will%20be%20required,especially%20in%20water%2Dstressed%20areas, last access: 10/7/2024, 2024.

Ehalt Macedo, H., Lehner, B., Nicell, J., Grill, G., Li, J., Limtong, A., and Shakya, R.: Distribution and characteristics of wastewater treatment plants within the global river network, *Earth Syst. Sci. Data*, 14, 559–577, https://doi.org/10.5194/essd-14-559-2022, 2022.

Eilander, D., Winsemius, H. C., Van Verseveld, W., Yamazaki, D., Weerts, A., and Ward, P. J.: MERIT Hydro IHU [Dataset]. https://doi.org/10.5281/zenodo.5166932, 2020.

Elnashar, A., Wang, L., Wu, B., Zhu, B., and Zeng, H.: Synthesis of global actual evapotranspiration from 1982 to 2019. *Earth Systems Science Data*, 13(2): 447-480. https://doi.org/10.5194/essd-2020-124, 2021.

Fick, S. E., and Hijmans, R. J.: WorldClim 2: new 1-km spatial resolution climate surfaces for global land areas. *International Journal of Climatology*, *37*(12), 4302–4315. https://doi.org/10.1002/joc.5086, 2017.

Fridman, D., Biran, N., & Kissinger, M.: Beyond blue: An extended framework of blue water footprint accounting. *Science of The Total Environment*, *777*, 146010. https://doi.org/10.1016/j.scitotenv.2021.146010, 2021.

Fridman, D., Kahil, T., and Wada, Y. Evaluating the global wastewater's untapped irrigation potential. *EGU General Assembly Conference Abstracts*, 2023.

Friedl, M. and Sulla-Menashe, D.: MCD12Q1 MODIS/Terra+Aqua land cover type yearly L3 Global 500m SIN Grid V006 NASA EOSDIS Land Processes DAAC [Dataset], 2019.

Graham, D. J., Bierkens, M. F., and van Vliet, M. T. Impacts of droughts and heatwaves on river water quality worldwide. *Journal of Hydrology*, 629, 130590. https://doi.org/10.1016/j.jhydrol.2023.130590, 2024.

Guillaumot, L., Smilovic, M., Burek, P., Bruijn, J. de, Greve, P., Kahil, T., and Wada, Y.: Coupling a large-scale hydrological model (CWatM) with a high-resolution groundwater flow model to assess the impact of irrigation at regional scale. *Geoscientific Model Development Discussions*, *2022*, 1–37. https://doi.org/10.5194/gmd-2022-161, 2022.

Israeli Government portal.: Desalination volumes by year. https://www.gov.il/BlobFolder/reports/desalination-stractures/he/%D7%9E%D7%AA%D7%A7%D7%99%20%D7%94%D7%AA%D7%A4%D7%9C%D7%94%20%D7%91%D7%99%D7%A9%D7%A8%D7%90%D7%9C.pdf, last accessed: 1/4/2022, 2022.

Israel Meteorological Service (IMS). Meteorological Databases. https://ims.gov.il/en/data_gov, last accessed: 1-10-2024, 2024.

Hamaarag.: Vegetation map of Israel's natural and forested areas, 2017. https://hamaarag.org.il, last accessed: 1-4-2022 , 2017.

Hanasaki, N., Matsuda, H., Fujiwara, M., Hirabayashi, Y., Seto, S., Kanae, S., and Oki, T.: Toward hyper-resolution global hydrological models including human activities: application to Kyushu island, Japan. *Hydrology and Earth System Sciences*, *26*(8), 1953–1975. https://doi.org/10.5194/hess-26-1953-2022, 2022.

Hoch, M. J., Sutanudjaja, E. H., Wanders, N., van Beek, R. L. P. H., and Bierkens, M. F. P.: Hyper-resolution PCR-GLOBWB: opportunities and challenges from refining model spatial resolution to 1 km over the European continent. *Hydrol. Earth Syst. Sci.*, 27: 1383-1401. https://doi.org/10.5194/hess-27-1383-2023, 2023.

688   ICBS.:   Municipal   data   in   Israel   1999-2021   [Dataset].

689   https://www.cbs.gov.il/he/publications/Pages/2019/%D7%94%D7%A8%D7%A9%D7%95%D7%99%D7%95

690   %D7%AA-%D7%94%D7%9E%D7%A7%D7%95%D7%9E%D7%99%D7%95%D7%AA-

691   %D7%91%D7%99%D7%A9%D7%A8%D7%90%D7%9C-%D7%A7%D7%95%D7%91%D7%A6%D7%99-

692   %D7%A0%D7%AA%D7%95%D7%A0%D7%99%D7%9D-

693   %D7%9C%D7%A2%D7%99%D7%91%D7%95%D7%93-1999-2017.aspx, last accessed: 14/2022, 2022.

694   INRA.: Wastewater collection, treatment, and recalmation for irrigation purposes – a national survey 2014.

695   https://www.google.com/url?sa=t&rct=j&q=&esrc=s&source=web&cd=&cad=rja&uact=8&ved=2ahUKEwimn

696   9aF7Z6GAxXRBdsEHTj0DEwQFnoECBIQAQ&url=https%3A%2F%2Fwww.gov.il%2FBlobFolder%2Frepor

697   ts%2Ftreated_waste_water1%2Fhe%2Fwater-sources-

698   status_kolhin_kolhim_2014.pdf&usg=AOvVaw3RjSAodJvw9NF0XD9h6qWY&opi=89978449, last accessed:

699   1/4/2022, 2016.

700   Israel Hydrological Services.: Hydrologic data - Annual report - The state of the water resources 2014.

701   https://www.gov.il/he/departments/publications/reports/water-resources-2014, last accessed: 1/4/2022, 2014.

702   Jones, E. R., Bierkens, M. F. P., Wanders, N., Sutanudjaja, E. H., van Beek, L. P. H., and van Vliet, M. T. H.:

703   DynQual v1.0: A high-resolution global surface water quality model. *Geoscientific Model Development*

704   *Discussions*, *2022*, 1–24. https://doi.org/10.5194/gmd-2022-222, 2022.

705   Jones, E. R., van Vliet, M. T. H. van, Qadir, M., and Bierkens, M. F. P.: Country-level and gridded estimates of

706   wastewater production, collection, treatment and reuse. *Earth System Science Data*, *13*(2), 237–254.

707   https://doi.org/10.5194/essd-13-237-2021, 2021.

708   Kim, Y., Park, H., Kimball, J. S., Colliander, A., and McCabe, M. F. Global estimates of daily evapotranspiration

709   using SMAP surface and root-zone soil moisture. *Remote Sensing of Environment*, 289: 113803.

710   https://doi.org/10.1016/j.rse.2023.113803, 2023.

711   Lange, S., Mengel, M., Treu, S., and Büchner, M.: ISIMIP3a atmospheric climate input data. ISIMIP Repository

712   [Dataset]. https://doi.org/10.48364/ISIMIP.982724, 2022.

713   Liao, X., Tian, Y., Gan, Y., and Ji, .J.: Quantifying urban wastewater treatment sector's greenhouse gas emissions

714   using a hybrid life cycle analysis method – An application on Shenzhen city in China. *Science of The Total*

715   *Environment*, 735: 141176. https://doi.org/10.1016/j.scitotenv.2020.141176, 2020.

716   Melloul, A., Albert, J., and Collin, M.: Lithological Mapping of the Unsaturated Zone of a Porous Media Aquifer

717   to Delineate Hydrogeological Characteristic Areas: Application to Israels Coastal aquifer. *African Journal of*

718   *Agricultural Research*, *1*(3), 47–56, 2006.

719   Meron, N., Blass, V., and Thoma, G.: A national-level LCA of a water supply system in a Mediterranean semi-

720   arid climate—Israel as a case study. *Int J Life Cycle Assess* 25, 1133–1144. https://doi.org/10.1007/s11367-020-

721   01753-5, 2020.

722   Ministry of Agriculture and Rural Development of Israel (MOAG).: Cultivated lands map, online GIS resource

723   [Dataset].https://data1-

724   moag.opendata.arcgis.com/datasets/f2cbce5354024da28f93788c53b182d2_0/explore?location=31.747323%2C3

725   4.905146%2C12.88, last accessed: 1/4/2022, 2022.

Moriasi, D. N., Gitau, M. W., Pai, N., and Daggupati, P.: Hydrologic and water quality models: Performance measures and evaluation criteria. *Transactions of the ASABE*, 58(6), 1763-1785. https://www.doi.org/10.13031/trans.58.10715, 2015.

Mu, Q., Maosheng, Z. Running, S. W., and Numerical Terradynamic Simulation Group.: MODIS Global terrestrial evapotranspiration (ET) product MOD16A2 collection 5 [Dataset], 2014.

Neitsch, S. L., Arnold, J. G., Kiniry, J. R., and Williams, J. R.: Soil and water assessment tool - Theoretical documentation - Version 2009. Texas Water Resources Institute, 2011.

OpenStreetMap contributors. (2022). Planet dump retrieved from https://planet.osm.org.

PCBS.: Water statistics in Palestinian territory 2001-2008 [Dataset]. https://www.pcbs.gov.ps/PCBS_2012/Publications.aspx?CatId=33&scatId=312, last accessed: 1/4/2022, 2022.

PCBS.: Wastewater statistics in Palestinina territory. https://www.pcbs.gov.ps/PCBS_2012/Publications.aspx?CatId=33&scatId=312, last accessed: 1/4/2022, 2022a.

Pescod, M. B.: Wastewater treatment and use in agriculture - FAO irrigation and drainage paper 47, 1992.

Reichle, R.H., De Lannoy, G., Koster, R.D., Crow, W.T., Kimball, J.S., Liu, Q., and Bechtold, M.: SMAP L4 Global 3-hourly 9 km EASE-Grid Surface and Root Zone Soil Moisture Analysis Update, Version 7. [Indicate subset used]. Boulder, Colorado USA. NASA National Snow and Ice Data Center Distributed Active Archive Center. doi:10.5067/LWJ6TF5SZRG3, 2022.

Rodell, M., Houser, P.R., Jambor, U., Gottschalck, J., Mitchell, K., Meng, C.-J., Arsenault, K., Cosgrove, B. , Radakovich, J., Bosilovich, M., Entin, J.K., Walker, J.P., Lohmann, D., and Toll, D..: The Global Land Data Assimilation System, *Bull. Amer. Meteor. Soc.*, 85(3), 381-394. https://doi.org/10.1175/BAMS-85-3-381, 2004.

Salvadore, E., Bronders, J., and Batelaan, O.: Hydrological modeling of urbanized catchments: A review and future directions. *Journal of Hydrology*, *529*, 62–81. https://doi.org/10.1016/j.jhydrol.2015.06.028, 2015.

Shangguan, W., Hengl, T., Jesus, J. Mendes de, Yuan, H., and Dai, Y. Mapping the global depth to bedrock for land surface modeling. *Journal of Advances in Modeling Earth Systems*, *9*(1), 65–88. https://doi.org/10.1002/2016MS000686, 2017.

Smilovic, M., Burek, P., Fridman D., Guillaumot, L., de Bruijn, J., Greve, P., Wada, Y., Tang, T., Kronfuss, M., and Hanus, S.: Water circles-a tool to assess and communicate the water cycle. *Environ. Res. Lett.*, 19: 021003. https://doi.org/10.1088/1748-9326/ad18de, 2024.

Tal, A.: Seeking Sustainability: Israel's Evolving Water Management Strategy. *Science*, *313*(5790), 1081–1084. https://doi.org/10.1126/science.1126011, 2006.

Thebo, A. L., Drechsel, P., Lambin E. F., and Nelson, K. L.: A global, spatially-explicit assessment of irrigated croplands influenced by urban wastewater flows. *Env. Res. Lett.*, 12(7): 074008, https://doi.org/10.1088/1748-9326/aa75d1, 2017.

van Jaarsveld, B., Wanders, N., Sutanudjaja, E. H., Hoch, J., Droppers, B., Janzing, J., van Beek, R. L. P. H., and Bierkens, M. F. P.: A first attempt to model global hydrology at hyper-resolution, *EGUsphere* [preprint], https://doi.org/10.5194/egusphere-2024-1025, 2024.

van Vliet, M. T. H., Jones, E. R., Flörke, M., Franssen, W. H. P., Hanasaki, N., Wada, Y., and Yearsley, J. R.: Global water scarcity including surface water quality and expansions of clean water technologies. *Env. Res. Lett.*, 16: 024020. https://doi.org/10.1088/1748-9326/abbfc3, 2021.

Wada, Y., Bierkens, M. F. P., Roo, A. de, Dirmeyer, P. A., Famiglietti, J. S., Hanasaki, N., Konar, M., Liu, J., Müller Schmied, H., Oki, T., Pokhrel, Y., Sivapalan, M., Troy, T. J., van Dijk, A. I. J. M.,van Emmerik, T., van Huijgevoort, M. H. J., van Lanen, H. A. J., Vörösmarty, C. J., Wanders, N., and Wheater, H.: Human–water interface in hydrological modeling: current status and future directions. *Hydrology and Earth System Sciences*, *21*(8), 4169–4193. https://doi.org/10.5194/hess-21-4169-2017, 2017

Wang, C., Song, J., Nunes, L. M., Zhao, H., Wang, P., Liang, Z., Arp, H. P. H., Li, G. and Xing, B. Global microplastic fiber pollution from domestic laundary. *Journal of Hazardous Materials*, 577, 135290. https://doi.org/10.1016/j.jhazmat.2024.135290, 2024.

Water Environment Federation (WEF): Clarifier design, Second edition. Manual of Practice No. FD-8. Water Environment Federation, 2005.

Wollmann, S., Calvo, R., and Burg, A.: A three-dimensional two-layers model to explore the hydrologic consequences of uncontrolled groundwater abstraction at Yarkon-Taninim Aquifer - Final report. https://www.gov.il/he/departments/publications/reports/wollman-et-al-report-2009, last accessd: 1/4/2022, 2009.

Yamazaki, D., Ikeshima, D., Tawatari, R., Yamaguchi, T., O'Loughlin, F., Neal, J. C., Sampson, C. C., Kanae, S., and Bates, P. D.: A high accuracy map of global terrain elevations. *Geophysical Research Letters*, *44*, 5844–5853. https://doi.org/10.1002/2017GL072874, 2017.Yang, W., Long, D., Scanlon, B. R., Burek, P., Zhang, C., Han, Z., Butler Jr., J. J., Pan, Y., Lei, X., and Wada, Y.: Human intervention will stabilize groundwater storage across the North China Plain. *Water Resources Research*, 58, e2021WR030884. https://doi.org/10.1029/2021WR030884, 2022.

Zhang, K., Kimball, J. S., and Running, S. W.: A review of remote sensing based actual evapotranspiration estimation. *WIREs Water*, 3: 834-853. https://doi.org/10.1002/wat2.1168, 2016.